FRASA: Feedback Retransmission Approximation for the Stability Region of Finite-User Slotted ALOHA

Ka-Hung Hui, On-Ching Yue and Wing-Cheong Lau
Department of Information Engineering
The Chinese University of Hong Kong,
Shatin, Hong Kong
Email: {khhui5, onching, wclau}@ie.cuhk.edu.hk

***Abstract*—We propose FRASA, *Feedback Retransmission Approximation for Slotted ALOHA*, to study the stability region of finite-user slotted ALOHA under collision channel. With FRASA, we derive in *closed form* the boundary of the stability region for *any* number of users in the system. The results derived from FRASA is identical to the analytical results of finite-user slotted ALOHA when there are two users. Simulation shows that the stability region obtained from FRASA is a good *approximation* to the stability region of finite-user slotted ALOHA. FRASA also has a wider range of applicability than the bounds derived in previous researches. We provide a *convex hull bound*, which is convex, piecewise linear and outer-bounds the stability region of FRASA. This bound can be obtained by using the transmission probability vector only. We also characterize p-*convexity*, an essential property that the stability region of FRASA should have to ensure the convex hull bound to be close to the boundary. From these, the stability region of FRASA can never be convex when there are more than two users. A separate convex and piecewise linear inner bound on the stability region of FRASA, *the supporting hyperplane bound*, is also given. The analytical findings with FRASA can also provide more insights on the characterization of the capacity region of other types of wireless random access networks.**

I. Introduction / Motivation

In the study of *wireless mesh networks*, one important performance measure is the capacity of the network when the effects of inter-link interference are considered. In particular, many researchers have focused on the design of *interference-aware routing / traffic engineering algorithms* to optimize the capacity of wireless mesh networks [1]–[3]. However, most of these works assume the existence of an ideal scheduler which can, in a centralized manner, coordinate and control link-level access of different nodes across the network. In contrast, practical wireless networks pre-dominantly use distributed *random access* protocols. The ability to characterize the capacity region of wireless random access networks has therefore become a pre-requisite for traffic engineering / optimization of such networks. Due to the complexity of the prevalent 802.11 MAC protocol, the analytical characterization of the capacity region of general 802.11-based networks seems to be forbiddenly intractable [4]. We therefore choose to study slotted-ALOHA-based networks instead, in order to gain insights on the capacity region and thus, the design of interference-aware traffic engineering algorithms for general wireless random access networks.

The study of the stability region of slotted ALOHA has attracted many researchers [5]–[13]. Despite the simplicity of slotted ALOHA, this problem is extremely difficult when M, the number of users in the system, exceeds two, even on the collision channel assumption. Under this assumption, successful transmissions occur if and only if there is one active transmitter, because of the interference among the stations. The inherent difficulty in the analysis is due to the effect of queueing in each transmitter. More specifically, the probability of successful transmission depends on the number of active transmitters, which in turn depends on whether the queues in the transmitters are empty or not. However, the stationary joint queue statistics still do not have closed form to date.

Instead of finding the exact stability region, previous researchers have attempted to bound the stability region [5]–[7], [10], [12]. However, they did not require the bounds to be *convex* or *piecewise linear*, which is important in traffic engineering. Requiring such property reduces the traffic engineering problem into convex or linear programming, which is easy to compute. Therefore, we are motivated to derive convex and piecewise linear bounds on the stability region. We hope this work can serve as a basis and can be extended to consider multi-hop networks and interference models other than collision channel.

In this paper, we propose FRASA, *Feedback Retransmission Approximation for Slotted ALOHA*, as a surrogate to approximate finite-user slotted ALOHA. By considering FRASA, we make the following contributions:

1) We obtain in *closed form* the boundary of the stability region of FRASA under collision channel for *any* number of users in Section III. The results obtained from FRASA are identical to the analytical results of finite-user slotted ALOHA for $M = 2$.
2) We demonstrate by simulation in Section IV that the stability region obtained from FRASA is a good approximation to the stability region of finite-user slotted ALOHA. We also demonstrate that FRASA has a wider range of applicability than the existing bounds.

3) In Section V we provide a *convex hull bound*, which is convex, piecewise linear and outer-bounds the stability region of FRASA. This bound can be computed by using the transmission probability vector only. In Section VI we introduce $\mathbf{p}$-*convexity*, which is essential to ensure the convex hull bound to be close to the boundary of the stability region of FRASA. The nonconvexity of the stability region of FRASA when $M > 2$ follows from these results.
4) A convex and piecewise linear inner bound on the stability region of FRASA, called the *supporting hyperplane bound*, is given in Section VII.

For the rest of the paper, we present related works in Section II. In Section VIII we conclude the paper and discuss future works.

II. Related Works

The study of the stability region of M-user infinite-buffer slotted ALOHA was initiated by [5] decades before, and is still an ongoing research. The authors in [5] obtained the exact stability region when $M = 2$ under collision channel. [6] and [7] used *stochastic dominance* and derived the same result as in [5] for the case of $M = 2$.

For general M, there were attempts to find the exact stability region, but there was only limited success. [9] established the boundary of the stability region, but it involves stationary joint queue statistics, which still do not have closed form to date. [13] obtained in closed form a partial characterization on the boundary of the stability region under *partial interference*.

Instead, many researchers focused on finding bounds on the stability region for general M. [5] obtained separate sufficient and necessary conditions for stability. [6] and [7] derived tighter bounds on the stability region by using stochastic dominance in different ways. [10] introduced *instability rank* and used it to improve the bounds on the stability region. However, the bounds in [6] and [10] are not always applicable. Also, the bounds obtained may not be piecewise linear.

With the advances in multi-user detection, researchers also studied this problem with the *multipacket reception* (MPR) model. [11] studied this problem in the infinite-user, single-buffer and symmetric MPR case. [12] considered the problem with finite users and infinite buffer. They obtained the boundary for the asymmetric MPR case with two users, and also the inner bound on the stability region for general M.

III. The FRASA Model

In slotted ALOHA, there is a queue of infinite buffer at each transmitter. Packet arrivals are assumed to be Bernoulli. When a packet arrives, it joins the end of the queue. The head-of-line packet is transmitted when the transmitter decides to transmit, and it remains at head-of-line until it is successfully transmitted. This is depicted in the upper part of Fig. 1.

Due to the complexity introduced by the queues, we propose FRASA, *Feedback Retransmission Approximation for Slotted ALOHA*, as a surrogate to approximate finite-user slotted ALOHA. In FRASA, the buffer in each transmitter can hold one packet only. Whenever there is a packet in the buffer, if the transmitter decides not to transmit the packet, or the transmitter cannot successfully transmit the packet due to collision, the packet will be removed from the buffer and put back in the buffer again after a random delay which is geometrically distributed. Therefore, the *aggregate arrival* of packets to the buffer, which is defined as the sum of the new arrivals and the retransmissions, is assumed to be Bernoulli or memoryless. Similar approximation was introduced by [14]. FRASA is shown in the lower part of Fig. 1.

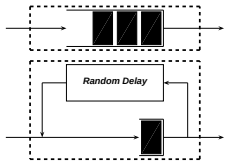

Fig. 1. Slotted ALOHA model: (Upper) Original; (Lower) FRASA.

Assume there are M links in the network, and the set of links is denoted by $\mathcal{M} = \{n\}_{n=1}^{M}$. Denote this FRASA system by $\overline{\mathsf{S}}$. Let $\mathbf{p} = (p_n)_{n\in\mathcal{M}}$ be the transmission probability vector. Define $\overline{p}_n = 1 - p_n$ for all $n \in \mathcal{M}$. We first consider a *reduced FRASA system*, in which we let $M - 1$ of the links have fixed aggregate arrival rates and the remaining link is assumed with infinite backlog. Take $\hat{n} \in \mathcal{M}$ to be the link with infinite backlog and denote this reduced FRASA system by $\overline{\mathsf{S}}_{\hat{n}}$. Let χ_n be the aggregate arrival rate of link $n \in \mathcal{M}\backslash\{\hat{n}\}$ where χ_n is between zero and one. Hence, link $\hat{n}$ is active with probability $p_{\hat{n}}$, while for $n \neq \hat{n}$, link n is active with probability $\chi_n p_n$. Therefore, $\overline{\boldsymbol{\lambda}} = \left(\overline{\lambda}_n\right)_{n\in\mathcal{M}}$ is the successful transmission probability vector and

$$\overline{\lambda}_n = \begin{cases} \chi_n p_n (1-p_{\hat{n}}) \displaystyle\prod_{n'\in\mathcal{M}\backslash\{n,\hat{n}\}} (1-\chi_{n'}p_{n'}), & n \neq \hat{n} \\ p_{\hat{n}} \displaystyle\prod_{n'\in\mathcal{M}\backslash\{\hat{n}\}} (1-\chi_{n'}p_{n'}), & n = \hat{n} \end{cases}, \tag{1}$$

with $\overline{\lambda}_{\hat{n}} > 0$. We use the results from [15] to determine when $\overline{\mathsf{S}}_{\hat{n}}$ is stable: on the assumption that the arrival and the service processes of a queue are stationary, the queue is stable if the average arrival rate is less than the average service rate, and the queue is unstable if the average arrival rate is larger than the average service rate. Then, $\lambda_n = \overline{\lambda}_n, \forall n \in \mathcal{M}$ is the *parametric form* of the boundary of the stability region of $\overline{\mathsf{S}}_{\hat{n}}$. We can obtain a non-parametric version by using (1) as follows.

Lemma 1: Consider $\overline{\mathsf{S}}_{\hat{n}}$. When

$$\frac{\lambda_{\hat{n}}(1-p_{\hat{n}})}{p_{\hat{n}}} \geq \frac{\lambda_n(1-p_n)}{p_n} \geq 0 \tag{2}$$

is satisfied for all $n \in \mathcal{M} \setminus \{\hat{n}\}$, the hypersurface $\mathsf{F}_{\hat{n}}$, *i.e.*,

$$\prod_{n'\in\mathcal{M}} [\lambda_{\hat{n}}(1-p_{\hat{n}}) + \lambda_{n'}p_{\hat{n}}] = p_{\hat{n}}[\lambda_{\hat{n}}(1-p_{\hat{n}})]^{M-1} \tag{3}$$

is the *non-parametric form* of the boundary of the stability region of $\overline{\mathsf{S}}_{\hat{n}}$.

Recall the system is stable if all queues in the system are stable [9], [10], [12], [13], and notice the expression $\frac{\lambda_n(1-p_n)}{p_n}$ in (2) is identical to the *instability rank* introduced in [10]. When $\max_{n\in\mathcal{M}} \frac{\lambda_n(1-p_n)}{p_n} = \frac{\lambda_{\hat{n}}(1-p_{\hat{n}})}{p_{\hat{n}}}$ holds as in (2), link $\hat{n}$ is the most probable one to be the first unstable link. Hence, we let link $\hat{n}$ to be infinitely backlogged and use Lemma 1 to obtain the stability region of FRASA as in the following Theorem.

Theorem 1: $\overline{\mathcal{R}} = \bigcup_{\hat{n}\in\mathcal{M}} \overline{\mathcal{R}}_{\hat{n}}$ is the stability region of FRASA, where $\overline{\mathcal{R}}_{\hat{n}}$ is represented by:

$$\frac{\lambda_{\hat{n}}(1-p_{\hat{n}})}{p_{\hat{n}}} \geq \frac{\lambda_n(1-p_n)}{p_n} \geq 0, \forall n \in \mathcal{M}\setminus\{\hat{n}\}, \quad (4)$$

$$\prod_{n'\in\mathcal{M}} [\lambda_{\hat{n}}(1-p_{\hat{n}}) + \lambda_{n'}p_{\hat{n}}] < p_{\hat{n}}[\lambda_{\hat{n}}(1-p_{\hat{n}})]^{M-1}. \quad (5)$$

The union here is actually a disjoint union.

We first illustrate our results for $M = 2$. When

$$\frac{\lambda_1(1-p_1)}{p_1} \geq \frac{\lambda_2(1-p_2)}{p_2} \geq 0$$

holds, the boundary of the stability region of FRASA is

$$\lambda_1[\lambda_1(1-p_1) + \lambda_2 p_1] = p_1\lambda_1(1-p_1),$$

which is reduced to

$$\lambda_1 = p_1\left(1 - \frac{\lambda_2}{1-p_1}\right)$$

after simplification. Geometrically, it is a straight line joining the points $(p_1, 0)$ and $(p_1\overline{p}_2, p_2\overline{p}_1)$. This is depicted in the bottom left of Fig. 2. By symmetry, we also get

$$\lambda_2 = p_2\left(1 - \frac{\lambda_1}{1-p_2}\right)$$

as the boundary of the stability region of FRASA when

$$\frac{\lambda_2(1-p_2)}{p_2} \geq \frac{\lambda_1(1-p_1)}{p_1} \geq 0$$

holds. This is a straight line joining the points $(0, p_2)$ and $(p_1\overline{p}_2, p_2\overline{p}_1)$. This is shown in the bottom center of Fig. 2. The bottom right of Fig. 2 contains the final result of the stability region obtained from FRASA. The stability region derived in [6] is illustrated in top row of Fig. 2 for comparison. We see that the final results are identical to each other.

Next we consider the case of $M = 3$ and each link has a transmission probability of 0.3. Figs. 3(a), 3(b) and 3(c) illustrate the results of Lemma 1 for $\overline{\mathsf{S}}_1$, $\overline{\mathsf{S}}_2$ and $\overline{\mathsf{S}}_3$ respectively. The single-colored hyperplanes in Figs. 3(a), 3(b) and 3(c) form the partition of the positive orthant generated by (2), while the multi-colored hypersurfaces come from (3). The union of these regions constitutes the stability region in Fig. 3(d) as stated in Theorem 1. Another example is shown in Figs. 4(a)-4(d), in which each link transmits with probability 0.6.

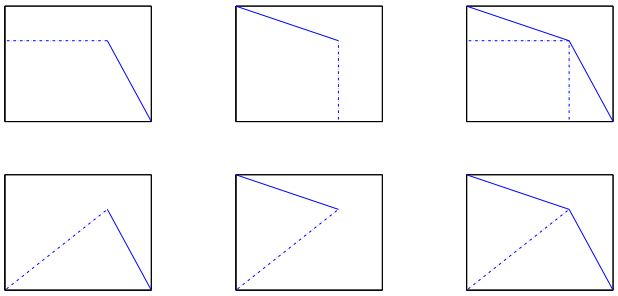

Fig. 2. Stability region with $M = 2$: (Upper) From [6] and [10]; (Lower) From FRASA.

IV. Validation of the FRASA Model

A. Simulation Results

In this section, we first use simulation to verify if FRASA is a good approximation to finite-user slotted ALOHA. Since when $M = 2$, we obtain identical results for both FRASA and finite-user slotted ALOHA, we consider $M = 3$ here.

To determine the boundary of the stability region, we use the following approach based on bisection method [16]. Given any $\mathbf{p} = (p_1, p_2, p_3)$, for any λ_1 and λ_2 between zero and one, let the initial search range of λ_3 be $[0, 1]$ and set λ_3 to be the midpoint of the search range. Then we let $\boldsymbol{\lambda} = (\lambda_1, \lambda_2, \lambda_3)$ be the arrival probabilities of the links and simulate the slotted ALOHA system. We use the algorithm proposed in [17] to check the stability of the queues in the system and conclude the stability of the system. This algorithm uses the statistics of the queue lengths to estimate the time-average of the growth rate of the queues. If the algorithm indicates that the system is stable, we set the next search range of λ_3 to be the upper half of the original one; otherwise, we use the lower half as the next search range. We iterate until the search range is sufficiently small. Then we take the midpoint of the final search range to be the boundary value of λ_3 for the given values of λ_1 and λ_2. We repeat this procedure for any combination of λ_1 and λ_2 to get the boundary of the stability region.

For illustrative purposes, we only show the cross-sections of the stability regions. We first let all links transmit with probability 0.3. In Fig. 5(a) we depict the cross-sections of the stability regions by fixing λ_2, while in Fig. 5(b) the cross-sections of the stability regions are obtained by fixing λ_1. The solid lines represent the simulation results while the dash-dot lines are obtained from FRASA. In Figs. 6(a) and 6(b) we show the corresponding results by changing the transmission probabilities of all links to 0.6. From these results, the stability region of FRASA can be regarded as a good approximation to the stability region of finite-user slotted ALOHA.

B. Comparison to Previous Bounds

Here, we demonstrate that FRASA is a good approximation to finite-user slotted ALOHA by showing the boundary values obtained from FRASA lie inside the upper and lower bounds in [10]. We fix the loading of the first $M-1$ links, evaluate

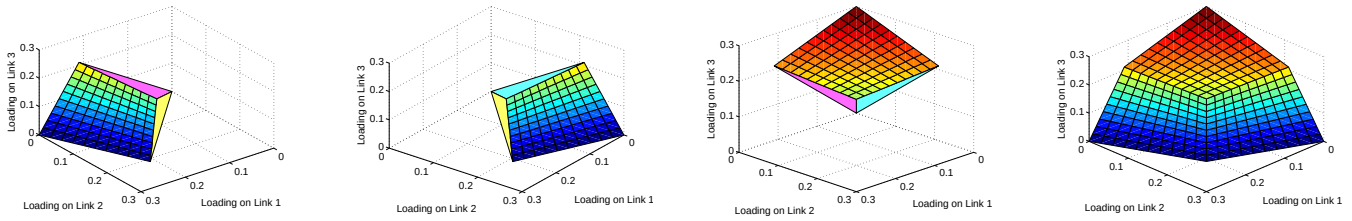

(a) (b) (c) (d)

Fig. 3. Stability region of FRASA with $M = 3$ and transmission probabilities 0.3 by Lemma 1 and Theorem 1: (a) $\overline{\mathcal{R}}_1$, stability region with link 1 having maximum instability rank; (b) $\overline{\mathcal{R}}_2$, stability region with link 2 having maximum instability rank; (c) $\overline{\mathcal{R}}_3$, stability region with link 3 having maximum instability rank; (d) $\overline{\mathcal{R}}$, the whole stability region.

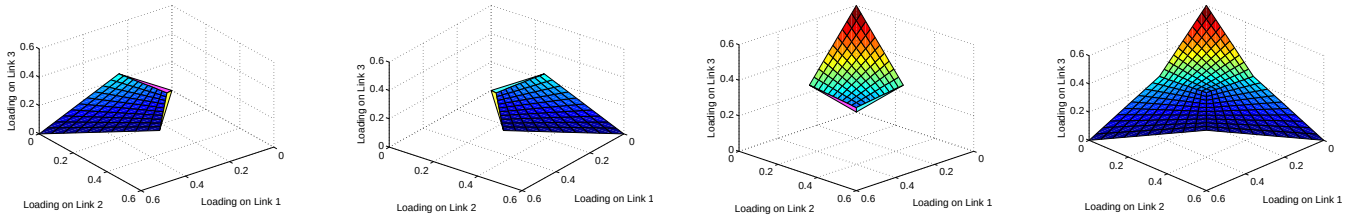

(a) (b) (c) (d)

Fig. 4. Stability region of FRASA with $M = 3$ and transmission probabilities 0.6 by Lemma 1 and Theorem 1: (a) $\overline{\mathcal{R}}_1$, stability region with link 1 having maximum instability rank; (b) $\overline{\mathcal{R}}_2$, stability region with link 2 having maximum instability rank; (c) $\overline{\mathcal{R}}_3$, stability region with link 3 having maximum instability rank; (d) $\overline{\mathcal{R}}$, the whole stability region.

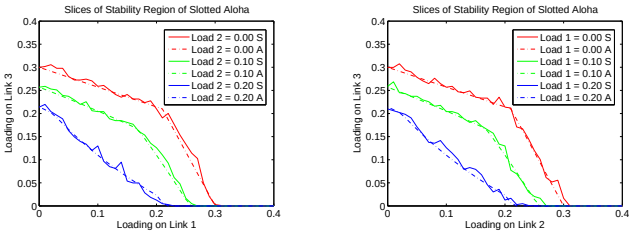

(a) (b)

Fig. 5. Cross-section of stability region with $M = 3$ and transmission probabilities 0.3: (a) λ_2 fixed, (b) λ_1 fixed.

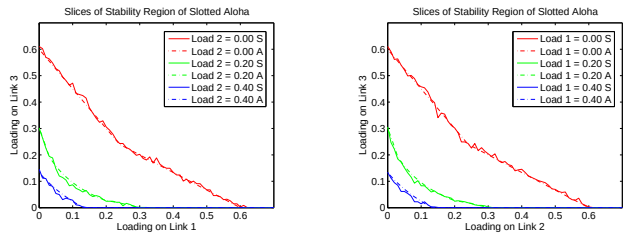

(a) (b)

Fig. 6. Cross-section of stability region with $M = 3$ and transmission probabilities 0.6: (a) λ_2 fixed, (b) λ_1 fixed.

the "Exact" value of λ_M from FRASA, and evaluate the "Upper" bound and "Lower" bound of λ_M by using Theorems 3 and 5 in [10] respectively. Before showing this, we point out that the bounds in [10] are applicable only when the instability rank assumption, *i.e.*, link M has the highest instability rank, holds. This is best illustrated by the following examples. Consider a slotted ALOHA system with two users. We let both links transmit with probability 0.6. We keep increasing λ_1 while assuming $\frac{\lambda_1(1-p_1)}{p_1} \leq \frac{\lambda_2(1-p_2)}{p_2}$, and evaluate the upper bound on λ_2 by using Theorem 3 in [10]. When $\lambda_1 > p_1\overline{p}_2$, the upper bound, *i.e.*, $\lambda_{2,\max}$, satisfies $\frac{\lambda_2(1-p_2)}{p_2} \leq \frac{\lambda_{2,\max}(1-p_2)}{p_2} < \frac{\lambda_1(1-p_1)}{p_1}$, showing that the instability rank assumption does not hold. We change the transmission probabilities of both links to 0.3 and repeat the whole process, but evaluate the lower bound on λ_2 by using Theorem 5 in [10]. It is found that when $\lambda_1 > p_1\overline{p}_2$, the lower bound, *i.e.*, $\lambda_{2,\min}$, satisfies $\frac{\lambda_{2,\min}(1-p_2)}{p_2} < \frac{\lambda_1(1-p_1)}{p_1}$, and we cannot conclude whether the instability rank assumption is valid or not. These results are depicted in Figs. 7(a) and 7(b) respectively. In the case of $M = 2$, we already have the complete characterization on the boundary of the stability region, therefore we can explicitly evaluate λ_2 and show that when $\lambda_1 > p_1\overline{p}_2$, the instability rank assumption does not hold, and the Theorems in [10] are not applicable. When $M > 2$, if there are some λ_n satisfying $\lambda_n > p_n \prod_{n' \in \mathcal{M}\setminus\{n\}} \overline{p}_{n'}$, it is difficult to predict whether the instability rank assumption is valid or not. When the instability rank assumption is not valid, one may tempt to switch the order of the links to keep the validity of the assumption. But in this case, we even cannot determine the stability of the links with instability ranks higher than that of link M, because the bounds on link n depend on

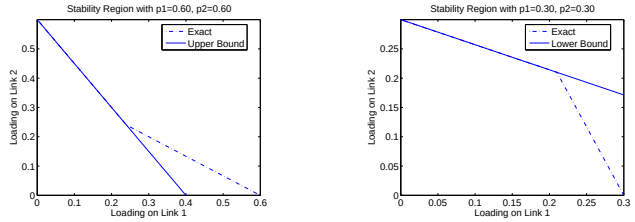

(a) (b)

Fig. 7. Restricted application of the upper and lower bounds in [10].

the loadings on the links having smaller instability ranks than link n [10]. Therefore, when using the bounds in [10], we cannot set the loadings on the first $M-1$ links too large in order to maintain the instability rank assumption.

However, there is no such restriction in computing the "Exact" value of λ_M from FRASA. We first let link M be the link with the highest instability rank, *i.e.*, $\hat{n}=M$. Then we solve (3) for λ_M, which is an equation of degree $M-1$, and get $M-1$ values of λ_M. Exactly one of them is the desired value, which makes the instability rank of link M the highest. Otherwise, we find the link with the highest instability rank among the first $M-1$ links. We let it equals $\hat{n}$ and solve (3) for λ_M, which is an equation of degree one. In this case, we get a nonnegative value which is the desired value of λ_M. Otherwise, we conclude that with the loadings on the first $M-1$ links, it is impossible to keep the system stable no matter how small λ_M is.

To compare the numerical values computed from FRASA against the bounds in [10], we consider the numerical examples in [6] and [10]. Due to space constraints, we only show the examples in [10], which are reproduced in Tables I-IV. The values of the loadings are classified into four groups in each table. In G1, one or more values of λ_n are zero. In G2, all λ_n are approximately equal to $\frac{1}{2}p_n\prod_{n'\in\mathcal{M}\setminus\{n\}}\overline{p}_{n'}$. In G3, all λ_n are close to $p_n\prod_{n'\in\mathcal{M}\setminus\{n\}}\overline{p}_{n'}$. In G4, one or more λ_n satisfy $\lambda_n > p_n\prod_{n'\in\mathcal{M}\setminus\{n\}}\overline{p}_{n'}$, and these λ_n are marked with asterisks in the tables. In all cases, the values predicted from FRASA lie inside the upper and lower bounds in [10]. Simulations are also performed for all examples in [6] and [10], and the results are shown in brackets in the tables. While the difference between the simulation result and the predicted value from FRASA can be as large as 40% (the first case of G4 in Table II), for most cases, 82 (resp. 90) out of 96, the simulation results are within $\pm 2\%$ (resp. $\pm 10\%$) from the values predicted from FRASA.

V. Convex Hull Bound

In this section, we develop an outer bound on the stability region of FRASA that is guaranteed to be convex and piecewise linear by using *corner points* of the stability region of FRASA. The definition of corner point is as follows. First we choose any $\hat{n}\in\mathcal{M}$. For any $\mathcal{M}'\subseteq\mathcal{M}\setminus\{\hat{n}\}$, we let χ_n have

TABLE I
Comparison for λ_M for $M=3$ and $p_1=p_2=p_3=0.5$.

	λ_1	λ_2	Upper	Exact (Simulation)	Lower
G1	0	0	0.5	0.5 (0.499596)	0.5
	0	0.12	0.38	0.38 (0.383064)	0.38
G2	0.06	0.06	0.38	0.370278 (0.365150)	0.340526
G3	0.12	0.123	0.257	0.17036 (0.158455)	0.140231
G4	0.12	0.13*	0.25	0.13 (0.131462)	0.13

TABLE II
Comparison for λ_M for $M=3$ and $p_1=0.6, p_2=0.7, p_3=0.8$.

	λ_1	λ_2	Upper	Exact (Simulation)	Lower
G1	0	0	0.8	0.8 (0.801918)	0.8
	0	0.05	0.6	0.6 (0.601158)	0.6
	0.03	0	0.68	0.68 (0.682747)	0.68
G2	0.018	0.028	0.616	0.602618 (0.593758)	0.508
G3	0.03	0.05	0.48	0.423303 (0.375008)	0.24
G4	0.035	0.0561*	0.4356	0.344373 (0.203636)	0.115187
	0.025	0.0563*	0.4748	0.421353 (0.359871)	0.277705

the following values for all $n\in\mathcal{M}\setminus\{\hat{n}\}$:

$$\chi_n=\begin{cases}1, & n\in\mathcal{M}'\\ 0, & n\in\mathcal{M}\setminus\left(\mathcal{M}'\cup\{\hat{n}\}\right)\end{cases}.$$

From this construction, for each $\mathcal{M}'$ we obtain a corner point $\Pi^{\mathsf{p}^{\mathcal{M}}(\mathcal{M}'\cup\{\hat{n}\})}=\left(\Pi_n^{\mathsf{p}^{\mathcal{M}}(\mathcal{M}'\cup\{\hat{n}\})}\right)_{n\in\mathcal{M}}$, where

$$\Pi_n^{\mathsf{p}^{\mathcal{M}}(\mathcal{M}'\cup\{\hat{n}\})}=\begin{cases}p_n\displaystyle\prod_{n'\in\mathcal{M}'\cup\{\hat{n}\}\setminus\{n\}}\overline{p}_{n'}, & n\in\mathcal{M}'\cup\{\hat{n}\}\\ 0, & n\notin\mathcal{M}'\cup\{\hat{n}\}\end{cases}. \tag{6}$$

These corner points, by construction, lie on the boundary of the stability region of FRASA because they satisfy the parametric form (1). We first obtain the following Lemma, stating the relationship between the boundary of the stability region of FRASA and the corner points.

Lemma 2: The boundary of the stability region of $\overline{\mathsf{S}}_{\hat{n}}$, *i.e.*, the hypersurface $\mathsf{F}_{\hat{n}}$, is contained in the convex hull $\mathsf{H}_{\hat{n}}$ generated by the corner points $\Pi^{\mathsf{p}^{\mathcal{M}}(\mathcal{M}'\cup\{\hat{n}\})}$ for all $\mathcal{M}'\subseteq\mathcal{M}\setminus\{\hat{n}\}$, *i.e.*, every point satisfying (3) is a convex combination of the corner points $\Pi^{\mathsf{p}^{\mathcal{M}}(\mathcal{M}'\cup\{\hat{n}\})}$ for all $\mathcal{M}'\subseteq\mathcal{M}\setminus\{\hat{n}\}$.

By using Lemma 2 and Theorem 1, we obtain the following Theorems about using convex hulls to bound the stability region of FRASA. To obtain the bounds from these Theorems, we only have to know the coordinates of all corner points, which can be computed from (6) based on the transmission probability vector only.

Theorem 2 (Bound of Convex-Hull Union): The convex hull generated by $\Pi^{\mathsf{p}^{\mathcal{M}}(\mathcal{M}'\cup\{\hat{n}\})}$ for all $\mathcal{M}'\subseteq\mathcal{M}\setminus\{\hat{n}\}$ together with $\mathbf{0}$, *i.e.*, the origin, is a piecewise linear outer bound on $\overline{\mathcal{R}}_{\hat{n}}$. Denote this convex hull by $\mathcal{H}_{\hat{n}}$. Therefore, the union of these $\mathcal{H}_{\hat{n}}$ for all $\hat{n}\in\mathcal{M}$, *i.e.*, $\overline{\mathcal{H}}=\bigcup_{\hat{n}\in\mathcal{M}}\mathcal{H}_{\hat{n}}$, is a piecewise linear outer bound on the stability region of FRASA. The union here is also disjoint.

Proof: Refer to Appendix A. ■

TABLE III
COMPARISON FOR λ_M FOR $M = 5$ AND $p_1 = p_2 = p_3 = p_4 = p_5 = 0.5$.

	λ_1	λ_2	λ_3	λ_4	Upper	Exact (Simulation)	Lower
G1	0	0	0	0	0.5	0.5 (0.499870)	0.5
	0	0	0	0.015	0.485	0.485 (0.487190)	0.485
	0	0	0.015	0.015	0.47	0.469521 (0.468605)	0.462021
	0	0.015	0.015	0.015	0.455	0.453495 (0.455147)	0.421588
G2	0.015	0.015	0.015	0.015	0.44	0.436838 (0.433372)	0.337257
G3	0.03	0.03	0.03	0.03	0.38	0.364349 (0.347664)	0.048165
G4	0.03	0.03	0.03	0.033*	0.377	0.360352 (0.343758)	0.045835
	0.033*	0.032*	0.031	0.03	0.374	0.356292 (0.330086)	0.039261
	0.0325*	0.032*	0.0315*	0.03	0.374	0.356289 (0.329231)	0.037718

TABLE IV
COMPARISON FOR λ_M FOR $M = 10$ AND $p_1 = p_2 = p_3 = p_4 = p_5 = p_6 = p_7 = p_8 = p_9 = p_{10} = 0.1$.

	λ_1	λ_2	λ_3	λ_4	λ_5	λ_6	λ_7	λ_8	λ_9	Upper	Exact (Simulation)	Lower
G1	0	0	0	0	0	0	0	0	0	0.1	0.1 (0.099754)	0.1
	0	0.019	0.019	0.019	0.019	0.019	0.019	0.019	0.019	0.083111	0.081498 (0.081612)	0.077453
G2	0.019	0.019	0.019	0.019	0.019	0.019	0.019	0.019	0.019	0.081	0.078832 (0.079277)	0.073177
G3	0.036	0.036	0.036	0.036	0.036	0.036	0.036	0.036	0.036	0.064	0.050075 (0.049960)	0.04286
G4	0.039*	0.036	0.036	0.036	0.036	0.036	0.036	0.036	0.036	0.063667	0.04913 (0.049294)	0.042554
	0.039*	0.039*	0.039*	0.039*	0.036	0.036	0.036	0.036	0.036	0.062667	0.045913 (0.046425)	0.041415

Theorem 3 (Convex Hull Bound): $\mathcal{H}$, the convex hull generated by $\Pi^{\mathbf{p}^{\mathcal{M}}(\mathcal{M}')}$ for all $\mathcal{M}' \subseteq \mathcal{M}$, is a convex and piecewise linear outer bound on the stability region of FRASA.

Theorem 3 follows immediately by noticing that $\mathcal{H}$ is the convex hull of $\overline{\mathcal{H}}$.

In finding the bounds on λ_M given the loadings on the other links, we do not have to rely on the instability rank assumption as in [10]. To apply Theorem 2, we first assume link M to have the highest instability rank, and generate the corresponding convex hull. If the assumption is valid, we can find a lower bound and an upper bound from the convex hull. Otherwise, we choose from the remaining links the link with the highest instability rank and repeat the process. Theorem 3 can be applied in any case in finding the upper bound.

We demonstrate the results from these Theorems in the following examples. Figs. 8(a), 8(b) and 8(c) illustrate the results of Theorem 2, assuming the transmission probabilities of all links are 0.3. The polytopes shown in these figures are the convex hulls $\mathcal{H}_1$, $\mathcal{H}_2$ and $\mathcal{H}_3$ generated by the corresponding corner points respectively. Fig. 8(d) shows $\overline{\mathcal{H}}$, the union of the convex hulls in Figs. 8(a), 8(b) and 8(c). Fig. 8(e) depicts $\mathcal{H}$, the convex hull generated by all corner points. The polytopes in Figs. 8(d) and 8(e) are identical. To show that this is not necessarily true, we give another example in which the transmission probabilities of all links are 0.6. In this example, $\overline{\mathcal{H}}$ in Fig. 9(d) is contained inside $\mathcal{H}$ in Fig. 9(e).

VI. $\mathbf{p}$-CONVEXITY

From the examples shown in previous section, the bounds on the stability region of FRASA obtained from Theorems 2 and 3, *i.e.*, $\overline{\mathcal{H}}$ and $\mathcal{H}$ respectively, need not be identical. Recall that both $\overline{\mathcal{H}}$ and $\mathcal{H}$ are completely characterized by the transmission probability vector only. Intuitively, for $\overline{\mathcal{H}} = \mathcal{H}$, we require $\overline{\mathcal{H}}$ to be a convex set, which means the transmission probability vector may need to satisfy some "convexity" conditions. In this section, we formalize these ideas and investigate the necessary and sufficient condition for $\overline{\mathcal{H}}$ and $\mathcal{H}$ to be identical.

We first define $\mathbf{p}$-convexity, and characterize the condition on the transmission probability vector for $\mathbf{p}$-convexity to hold.

Definition 1: We use the corner points $\Pi^{\mathbf{p}^{\mathcal{M}}(\mathcal{M}\setminus\{\bar{n}\})}$ for each $\bar{n} \in \mathcal{M}$ to form a hyperplane $\Omega^{\mathcal{M}}$. If the corner points $\Pi^{\mathbf{p}^{\mathcal{M}}(\mathcal{M})}$ and $\mathbf{0}$ lie on opposite sides of $\Omega^{\mathcal{M}}$, or $\Pi^{\mathbf{p}^{\mathcal{M}}(\mathcal{M})}$ lies on $\Omega^{\mathcal{M}}$, the stability region of FRASA is said to be $\mathbf{p}$-*convex*.

Theorem 4: The stability region of FRASA is $\mathbf{p}$-convex if and only if

$$\sum_{n\in\mathcal{M}} p_n \leq 1. \tag{7}$$

The $\mathbf{p}$-convexity of the stability region of FRASA can be regarded as a measure of contention level in the system. p_n can be viewed as the proportion of time that link n is active. $\sum_{n\in\mathcal{M}} p_n \leq 1$ represents the case that the increase in channel utilization outweighs the increase in contention due to addition of one more link to the system. This is possible because when the channel utilization is small, the probability that a new link choose an idle time slot to transmit is large, therefore the contention introduced by this new link will be small and the stability region of FRASA will be $\mathbf{p}$-convex. On the other hand, if $\sum_{n\in\mathcal{M}} p_n > 1$, the contention level will be so large that it is not beneficial to introduce one more link to the system. Even in the ideal case, *i.e.*, TDMA with perfect scheduling, it is impossible to assign time slots to the links such that there is no contention. Hence, contention is inevitable in this situation, and the stability region of FRASA will not be $\mathbf{p}$-convex. Consequently, it is undesirable to allow the links to be active with probability p_n.

From (7), we observe that to make the stability region to be $\mathbf{p}$-convex, the transmission probabilities of all links should be set according to the number of neighboring links in proximity.

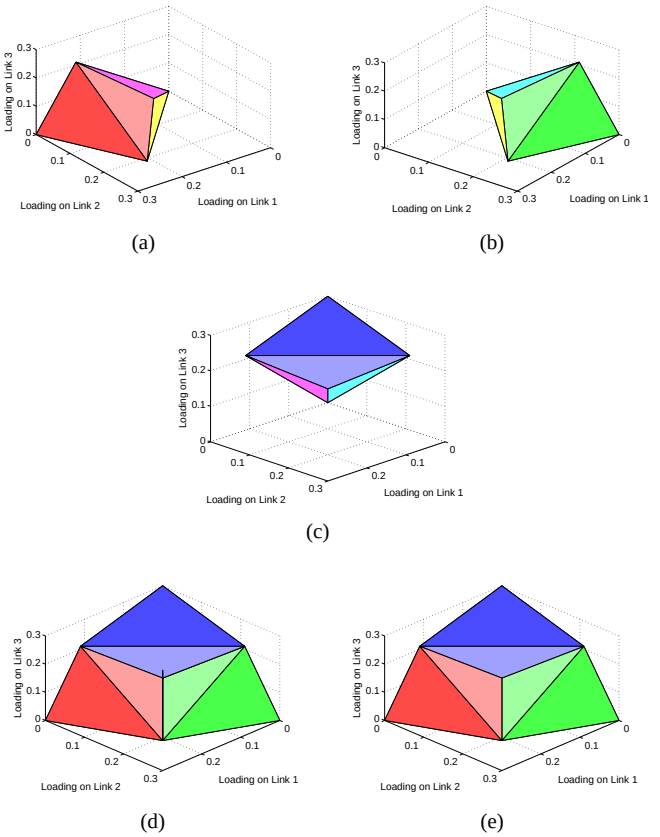

Fig. 8. Convex hull bound on stability region of FRASA with $M = 3$ and transmission probabilities 0.3 by Theorems 2 and 3: (a) $\mathcal{H}_1$, convex hull of $\mathcal{R}_1$; (b) $\mathcal{H}_2$, convex hull of $\mathcal{R}_2$; (c) $\mathcal{H}_3$, convex hull of $\mathcal{R}_3$; (d) $\overline{\mathcal{H}}$, bound of convex-hull union; (e) $\mathcal{H}$, convex hull bound.

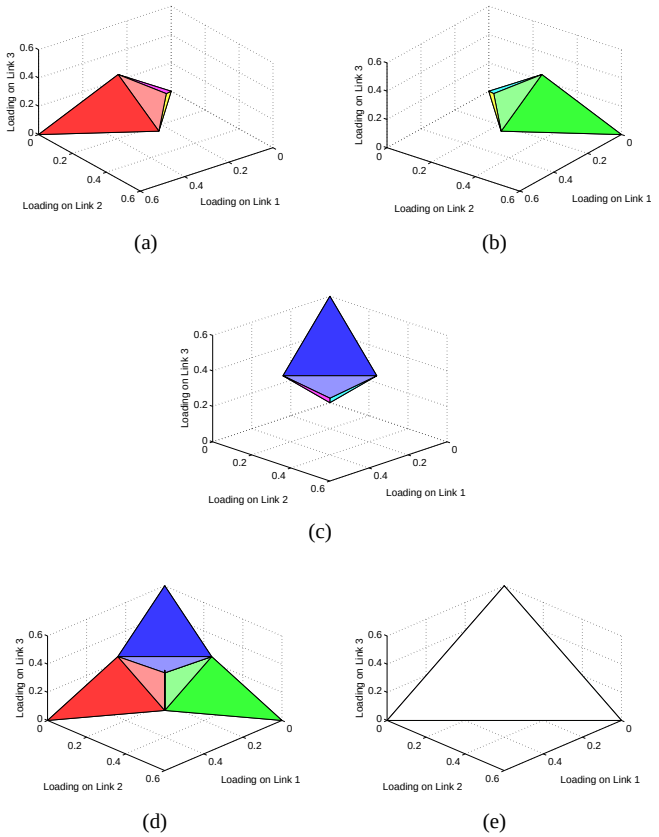

Fig. 9. Convex hull bound on stability region of FRASA with $M = 3$ and transmission probabilities 0.6 by Theorems 2 and 3: (a) $\mathcal{H}_1$, convex hull of $\mathcal{R}_1$; (b) $\mathcal{H}_2$, convex hull of $\mathcal{R}_2$; (c) $\mathcal{H}_3$, convex hull of $\mathcal{R}_3$; (d) $\overline{\mathcal{H}}$, bound of convex-hull union; (e) $\mathcal{H}$, convex hull bound.

For example, if we assume all links have the same priority, we may set each p_n to be $\frac{1}{M}$.

From Theorem 3, we know $\overline{\mathcal{H}} \subseteq \mathcal{H}$. We observe that if the stability region of FRASA with link set $\mathcal{M}$ is $\mathbf{p}$-convex, then the stability region of FRASA with link set $\mathcal{M}'$, where $\mathcal{M}' \subseteq \mathcal{M}$ and $|\mathcal{M}'| \geq 2$, is also $\mathbf{p}$-convex. It is because if (7) is satisfied, then $\sum_{n \in \mathcal{M}'} p_n \leq 1$ must be satisfied also. We now give a necessary and sufficient condition for the equality of $\overline{\mathcal{H}}$ and $\mathcal{H}$ based on this observation.

Theorem 5: $\overline{\mathcal{H}} = \mathcal{H}$ if and only if the stability region of FRASA is $\mathbf{p}$-convex.

Proof: Refer to Appendix B. ∎

From Theorems 4 and 5, we know that (7) guarantees the stability region of FRASA to be $\mathbf{p}$-convex. Then, can (7) assure the convexity of the stability region of FRASA? Recall Theorem 1 that the boundary of the stability region of FRASA consists of M hypersurfaces, *i.e.*, $\mathsf{F}_{\hat{n}}$ for all $\hat{n} \in \mathcal{M}$. Also, Lemma 2 says that for each $\hat{n} \in \mathcal{M}$, the hypersurface $\mathsf{F}_{\hat{n}}$ is contained inside the convex hull $\mathsf{H}_{\hat{n}}$. If (7) holds, we need an additional condition to guarantee the convexity of the stability region of FRASA: for all $\hat{n} \in \mathcal{M}$, $\mathsf{F}_{\hat{n}}$ is a hyperplane, meaning that $\mathsf{F}_{\hat{n}} = \mathsf{H}_{\hat{n}}$. This additional condition is satisfied when $M = 2$ as illustrated in section III. Therefore, for $M = 2$, $\mathbf{p}$-convexity is equivalent to convexity and (7) guarantees the convexity of the stability region of FRASA. However, this is not the case for $M > 2$ since if such a hyperplane exists for some $\hat{n}$, the boundary of the stability region of FRASA is linear in $\lambda_{\hat{n}}$, contradicting to the non-parametric form (3) that the boundary is of degree at least two in $\lambda_{\hat{n}}$ when $M > 2$. Hence, the nonconvexity of the stability region of FRASA when $M > 2$ follows.

Consider again the examples in Figs. 8 and 9. In Fig. 8, $\sum_{n \in \mathcal{M}} p_n = 0.9 \leq 1$, therefore the stability region is $\mathbf{p}$-convex and $\overline{\mathcal{H}} = \mathcal{H}$. On the other hand, in Fig. 9, $\sum_{n \in \mathcal{M}} p_n = 1.8 > 1$, and $\overline{\mathcal{H}} \subsetneq \mathcal{H}$. In other words, the convex hull bound is tighter if and only if the stability region is $\mathbf{p}$-convex. We remark that even if the stability region may not be $\mathbf{p}$-convex, the convex hull bound is still a valid convex and piecewise linear outer bound on the stability region of FRASA.

VII. Supporting Hyperplane Bound

In this section, we give a convex and piecewise linear inner bound on the stability region of FRASA by using *supporting hyperplanes*. Recall that a supporting hyperplane of a convex

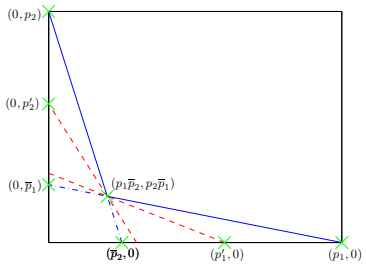

Fig. 10. Supporting hyperplane bound.

set is a hyperplane such that it intersects with the convex set and the convex set entirely belongs to only one of the closed half spaces generated by the hyperplane. This inner bound is obtained based on the result of Lemma 2.

Theorem 6 (Supporting Hyperplane Bound): For each $\hat{n} \in \mathcal{M}$, we construct a supporting hyperplane $\mathsf{P}_{\hat{n}}$ which supports the convex hull $\mathsf{H}_{\hat{n}}$ in Lemma 2 at $\Pi^{\mathbf{p}^{\mathcal{M}}(\mathcal{M})}$ such that

1) it lies below $\mathsf{H}_{\hat{n}}$; and
2) it has positive intercepts on all coordinate axes.

We let $\mathcal{S}_{\hat{n}}$ be the closed half space below $\mathsf{P}_{\hat{n}}$. Then the intersection of all these half spaces in the positive orthant, *i.e.*, $\mathcal{S} = \bigcap_{\hat{n}\in\mathcal{M}} \mathcal{S}_{\hat{n}} \cap \{\boldsymbol{\lambda}\colon \lambda_n \geq 0, \forall n \in \mathcal{M}\}$, is a convex and piecewise linear inner bound on the stability region of FRASA.

Proof: Refer to Appendix C. ∎

Consider the case that $M = 2$ as in Fig. 10. First we choose the hyperplanes as stated in Theorem 6. Specifically, the line segment between $(p_1, 0)$ and $(p_1\overline{p}_2, p_2\overline{p}_1)$ is the convex hull H_1. Then we choose any point $(p_1', 0)$ on λ_1-axis such that $p_1\overline{p}_2 \leq p_1' \leq p_1$ and form the hyperplane P_1, *i.e.*, the line passing through $(p_1', 0)$ and $(p_1\overline{p}_2, p_2\overline{p}_1)$. Similarly, we choose a point $(0, p_2')$ on λ_2-axis such that $p_2\overline{p}_1 \leq p_2' \leq p_2$ and form the hyperplane P_2. These hyperplanes are shown as the red dashed lines in Fig. 10. The intersection of the closed half spaces below the red lines in the positive quadrant is the inner bound from Theorem 6.

This supporting hyperplane bound is arbitrary, in the sense that for each $\hat{n} \in \mathcal{M}$, as long as the hyperplane constructed satisfies the requirements listed, $\mathcal{S}$ will be an inner bound. If we require the inner bound to occupy the maximum hypervolume, then this problem is equivalent to finding a maximum-hypervolume convex subset of the stability region of FRASA. To the best of our knowledge, this is studied only for $M = 2$ [18]. In this case, the problem is to find the maximum-area convex subset of a polygon. We recall some related definitions. A *reflex vertex* is a vertex of a polygon such that the angle at the vertex inside the polygon is reflex. A *chord* is a maximal line segment contained in the polygon.

First we consider the case that $p_1 + p_2 > 1$, *i.e.*, the stability region of FRASA is not $\mathbf{p}$-convex. In this case, as depicted in Fig. 10, the reflex vertex is $(p_1\overline{p}_2, p_2\overline{p}_1)$. By calculus, the maximum-hypervolume convex subset is either the region below the chord between $(p_1, 0)$ and $(0, \overline{p}_1)$, or the region below the chord between $(0, p_2)$ and $(\overline{p}_2, 0)$, depending on the values of p_1 and p_2. This is a special case of the result in [18]. Suppose the region below the chord between $(p_1, 0)$ and $(0, \overline{p}_1)$ is the maximum-hypervolume convex subset of the stability region of FRASA. If we partition this chord about $(p_1\overline{p}_2, p_2\overline{p}_1)$, we obtain two line segments: one of these lies on a supporting hyperplane of the boundary between $(p_1, 0)$ and $(p_1\overline{p}_2, p_2\overline{p}_1)$, while the other lies on a supporting hyperplane of the boundary between $(0, p_2)$ and $(p_1\overline{p}_2, p_2\overline{p}_1)$. Similar observations can also be found when the region below the chord between $(0, p_2)$ and $(\overline{p}_2, 0)$ is the maximum-hypervolume convex subset of the stability region of FRASA. This means when the stability region is not $\mathbf{p}$-convex, if we require the inner bound to have the maximum hypervolume, the supporting hyperplanes we need in Theorem 6 coincide.

On the other hand, if the stability region of FRASA is $\mathbf{p}$-convex, as stated in previous section, $\mathbf{p}$-convexity is equivalent to convexity. When $p_1 + p_2 \leq 1$, the stability region is $\mathbf{p}$-convex and also convex, and the stability region itself is the maximum-hypervolume convex subset. In this case, the line segments of the boundary are already the supporting hyperplanes we need.

VIII. Conclusion

In this paper, we proposed FRASA, Feedback Retransmission Approximation for Slotted ALOHA, to serve as a surrogate to approximate finite-user slotted ALOHA. From FRASA, we obtained in closed form the exact stability region for any number of users in the system under collision channel. We illustrated that the results from FRASA are identical to the analytical results of finite-user slotted ALOHA when there are two users. Simulation showed that the stability region obtained from FRASA is a good approximation to the stability region of finite-user slotted ALOHA. We demonstrated that our results from FRASA has a wider range of applicability than the existing bounds. We also established a convex hull bound, which is convex, piecewise linear and outer-bounds the stability region of FRASA. This convex hull bound can be generated by using the transmission probability vector only. We introduced $\mathbf{p}$-convexity, which is essential to ensure the convex hull bound to be close to the boundary of the stability region of FRASA. From these results, we deduced that the stability region of FRASA is nonconvex when there are more than two users. A separate convex and piecewise linear inner bound, supporting hyperplane bound, was also introduced.

We have only considered the stability of slotted ALOHA under collision channel. The collision channel assumption may not always hold, because the interference among stations may not be large enough to corrupt the packet receptions when the stations are spaced far away. We may extend our work to take into account the signal-to-noise ratio and consider different types of interference models. The model in this paper only covers the case of single-hop networks. Therefore, another possible extension is to consider the generalization of this work to multi-hop wireless networks. Also, extending the results on maximum-area convex subsets to cover the case of more than two users helps providing a better inner bound on

the stability region of FRASA. The stability region of FRASA, the convex hull bound and the supporting hyperplane bound obtained may be used in designing interference-aware traffic engineering algorithms in wireless random access networks.

APPENDIX

A. Proof of Theorem 2

Consider the reduced FRASA system $\overline{\mathsf{S}}_{\hat{n}}$ and let $\mathcal{M}' \subseteq \mathcal{M} \setminus \{\hat{n}\}$. From (6), for every $n \in \mathcal{M} \setminus \{\hat{n}\}$, all corner points $\Pi^{\mathsf{P}^{\mathcal{M}}(\mathcal{M}' \cup \{\hat{n}\})}$ with $n \in \mathcal{M}'$ and $\mathbf{0}$ lie on the boundary $\frac{\lambda_{\hat{n}}(1-p_{\hat{n}})}{p_{\hat{n}}} = \frac{\lambda_n(1-p_n)}{p_n}$, all corner points $\Pi^{\mathsf{P}^{\mathcal{M}}(\mathcal{M}' \cup \{\hat{n}\})}$ with $n \notin \mathcal{M}' \cup \{\hat{n}\}$ and $\mathbf{0}$ lie on the boundary $\frac{\lambda_n(1-p_n)}{p_n} = 0$. Also, for all $n \in \mathcal{M} \setminus \{\hat{n}\}$, the condition $0 \leq \chi_n \leq 1$ implies none of the corner points lie outside the region $\frac{\lambda_{\hat{n}}(1-p_{\hat{n}})}{p_{\hat{n}}} \geq \frac{\lambda_n(1-p_n)}{p_n} \geq 0$. Hence, for all $n \in \mathcal{M} \setminus \{\hat{n}\}$, $\frac{\lambda_{\hat{n}}(1-p_{\hat{n}})}{p_{\hat{n}}} = \frac{\lambda_n(1-p_n)}{p_n}$ and $\frac{\lambda_n(1-p_n)}{p_n} = 0$ are the boundaries of both $\overline{R}_{\hat{n}}$ and $\mathcal{H}_{\hat{n}}$. Therefore, from Lemma 2, $\overline{\mathcal{R}}_{\hat{n}} \subseteq \mathcal{H}_{\hat{n}}$, and $\overline{\mathcal{R}} = \bigcup_{\hat{n} \in \mathcal{M}} \overline{\mathcal{R}}_{\hat{n}} \subseteq \bigcup_{\hat{n} \in \mathcal{M}} \mathcal{H}_{\hat{n}} = \overline{\mathcal{H}}$. Since the boundaries $\frac{\lambda_{\hat{n}}(1-p_{\hat{n}})}{p_{\hat{n}}} = \frac{\lambda_n(1-p_n)}{p_n}$ and $\frac{\lambda_n(1-p_n)}{p_n} = 0$ are linear and the convex hull generated by a set of points is piecewise linear, $\overline{\mathcal{H}}$ is piecewise linear. ∎

B. Proof of Theorem 5

Notice that $\mathcal{H}$ is the convex hull of $\overline{\mathcal{H}}$. The corner points either lie on the boundary of $\mathcal{H}$ or in the interior of $\mathcal{H}$. If the stability region of FRASA is $\mathbf{p}$-convex, we only need to show that all corner points lie on the boundary of $\mathcal{H}$. It is because if all corner points are on the boundary of $\mathcal{H}$, then the union $\bigcup_{\hat{n} \in \mathcal{M}} \mathcal{H}_{\hat{n}}$ is convex and hence $\overline{\mathcal{H}} = \mathcal{H}$. Consider $M = 2$. When forming the convex hull $\mathcal{H}$, either

1) $\Pi^{\mathsf{P}^{\mathcal{M}}(\mathcal{M})}$ lies on $\Omega^{\mathcal{M}}$, meaning that $\Omega^{\mathcal{M}}$ is part of the boundary of $\mathcal{H}$; or
2) $\Pi^{\mathsf{P}^{\mathcal{M}}(\mathcal{M})}$ and $\mathbf{0}$ lie on opposite sides of $\Omega^{\mathcal{M}}$, which means $\Omega^{\mathcal{M}}$ will not be the boundary of $\mathcal{H}$ because there is a corner point $\Pi^{\mathsf{P}^{\mathcal{M}}(\mathcal{M})}$ lying beyond $\Omega^{\mathcal{M}}$.

In both cases, $\Pi^{\mathsf{P}^{\mathcal{M}}(\mathcal{M})}$ lies on the boundary of $\mathcal{H}$. For general values of M greater than two, we consider all $\mathcal{M}' \subseteq \mathcal{M}$ where $2 \leq |\mathcal{M}'| < M$ in ascending order of $|\mathcal{M}'|$. Because the stability region of FRASA with link set $\mathcal{M}'$ is also $\mathbf{p}$-convex, by repeating the arguments as above, we see that now all corner points except $\Pi^{\mathsf{P}^{\mathcal{M}}(\mathcal{M})}$ are on the boundary of $\mathcal{H}$ and $\Omega^{\mathcal{M}}$ is the boundary of the stability region farthest away from $\mathbf{0}$. Now we consider the corner point $\Pi^{\mathsf{P}^{\mathcal{M}}(\mathcal{M})}$. We can apply similar arguments as above to show that $\Pi^{\mathsf{P}^{\mathcal{M}}(\mathcal{M})}$ lies on the boundary of $\mathcal{H}$. Hence, $\overline{\mathcal{H}} = \mathcal{H}$. On the other hand, if the stability region of FRASA is not $\mathbf{p}$-convex, then $\Pi^{\mathsf{P}^{\mathcal{M}}(\mathcal{M})}$ lies in between $\mathbf{0}$ and $\Omega^{\mathcal{M}}$. Therefore, at least one corner point does not lie on the boundary of $\mathcal{H}$ and $\overline{\mathcal{H}} \subsetneq \mathcal{H}$. ∎

C. Proof of Theorem 6

Consider the bound of convex hull union $\overline{\mathcal{H}}$ in Theorem 2. Choose an arbitrary $\hat{n} \in \mathcal{M}$. When $\overline{\mathcal{H}}$ is intersected with the closed half space $\mathcal{S}_{\hat{n}}$, the resultant polytope does not contain the convex hull $\mathsf{H}_{\hat{n}}$ by construction. Therefore, this resultant polytope excludes the hypersurface $\mathsf{F}_{\hat{n}}$. We repeat this argument for all $\hat{n} \in \mathcal{M}$, then for all $\hat{n} \in \mathcal{M}$, the convex hull $\mathsf{H}_{\hat{n}}$ together with the hypersurface $\mathsf{F}_{\hat{n}}$ are removed. The boundary of the resultant polytope is consisted of $\mathsf{P}_{\hat{n}}$ for all $\hat{n} \in \mathcal{M}$ and the boundary of the positive orthant only, and hence the polytope is $\mathcal{S}$. Therefore, $\mathcal{S}$ is a subset of $\overline{\mathcal{R}}$ and constitutes an inner bound on the stability region of FRASA. This bound is convex and piecewise linear since half spaces are convex and piecewise linear, and these two properties are preserved under intersection. ∎

REFERENCES

[1] K. Jain, J. Padhye, V. Padmanabhan, and L. Qiu, "Impact of Interference on Multi-hop Wireless Network Performance," in *MobiCom 2003*, San Diego, California, USA, Sep. 2003.

[2] R. Gupta, J. Musacchio, and J. Walrand, "Sufficient Rate Constraints for QoS Flows in Ad-Hoc Networks," *Ad Hoc Networks*, 2006.

[3] M. Kodialam and T. Nandagopal, "Characterizing the Capacity Region in Multi-Radio Multi-Channel Wireless Mesh Networks," in *MobiCom 2005*, Cologne, Germany, Aug./Sep. 2005.

[4] K.-H. Hui, W.-C. Lau, and O.-C. Yue, "Characterizing and Exploiting Partial Interference in Wireless Mesh Networks," in *ICC 2007*, Glasgow, Scotland, Jun. 2007.

[5] B. S. Tsybakov and V. A. Mikhailov, "Ergodicity of a Slotted ALOHA System," *Probl. Inform. Transm.*, vol. 15, no. 4, pp. 73–87, 1979.

[6] R. R. Rao and A. Ephremides, "On the Stability of Interacting Queues in a Multiple-Access System," *IEEE Trans. Inf. Theory*, vol. 34, no. 5, pp. 918–930, Sep. 1988.

[7] W. Szpankowski, "Stability Conditions for Multidimensional Queueing Systems with Computer Applications," *Oper. Res.*, vol. 36, no. 6, pp. 944–957, Nov./Dec. 1988.

[8] V. Anantharam, "The Stability Region of the Finite-User Slotted ALOHA Protocol," *IEEE Trans. Inf. Theory*, vol. 37, no. 3, pp. 535–540, May 1991.

[9] W. Szpankowski, "Stability Conditions for Some Multiqueue Distributed Systems: Buffered Random Access Systems," *Adv. Appl. Probab.*, vol. 26, pp. 498–515, Jun. 1994.

[10] W. Luo and A. Ephremides, "Stability of N Interacting Queues in Random-Access Systems," *IEEE Trans. Inf. Theory*, vol. 45, no. 5, pp. 1579–1587, Jul. 1999.

[11] S. Ghez, S. Verdú, and S. C. Schwartz, "Stability Properties of Slotted Aloha With Multipacket Reception Capability," *IEEE Trans. Autom. Control*, vol. 33, no. 7, pp. 640–649, Jul. 1988.

[12] V. Naware, G. Mergen, and L. Tong, "Stability and Delay of Finite-User Slotted ALOHA With Multipacket Reception," *IEEE Trans. Inf. Theory*, vol. 51, no. 7, pp. 2636–2656, Jul. 2005.

[13] K.-H. Hui, W.-C. Lau, and O.-C. Yue, "Stability of Finite-User Slotted ALOHA under Partial Interference in Wireless Mesh Networks," in *PIMRC 2007*, Athens, Greece, Sep. 2007, to appear.

[14] S. S. Lam, "Store-and-Forward Buffer Requirements in a Packet Switching Network," *IEEE Trans. Commun.*, vol. 24, no. 4, pp. 394–403, Apr. 1976.

[15] R. M. Loynes, "The Stability of a Queue with Non-Independent Inter-arrival and Service Times," *Proc. Cambridge Phil. Soc.*, vol. 58, pp. 494–520, 1962.

[16] D. Kincaid and W. Cheney, *Numerical Analysis: Mathematics of Scientific Computing*, 3rd ed. Brooks/Cole, 2002.

[17] J. R. Wieland, R. Pasupathy, and B. W. Schmeiser, "Queueing-Network Stability: Simulation-Based Checking," in *Proceedings of the 2003 Winter Simulation Conference*, vol. 1, Dec. 2003, pp. 520–527.

[18] J.-S. Chang and C.-K. Yap, "A Polynomial Solution for Potato-Peeling and Other Polygon Inclusion and Enclosure Problems," in *25th Annual Symposium on Foundations of Computer Science*, Oct. 1984, pp. 408–416.